DNA methylation profiles differ in responders versus non-responders to anti-PD-1 immune checkpoint inhibitors in patients with advanced and metastatic head and neck squamous cell carcinoma

Angelika Martina Starzer [1,2] Gerwin Heller [1,2] Erwin Tomasich,[1,2] Thomas Melchardt,[3] Katharina Feldmann,[1,2] Teresa Hatziioannou,[1,2] Stefan Traint,[1] Christoph Minichsdorfer,[1] Ursula Schwarz-Nemec,[4] Maja Nackenhorst,[5] Leonhard Müllauer,[5] Matthias Preusser,[1,2] Anna Sophie Berghoff [1,2] Thorsten Fuereder[1]

Correspondence to
Dr Anna Sophie Berghoff; anna.berghoff@meduniwien.ac.at

ABSTRACT

Background Biomarkers for response prediction to anti-programmed cell death 1 (PD-1) immune checkpoint inhibitors (ICI) in patients with head and neck squamous cell carcinoma (HNSCC) are urgently needed for a personalized therapy approach. We investigated the predictive potential of inflammatory parameters and DNA methylation profiling in patients with HNSCC treated with anti-PD-1 ICI.

Methods We identified patients with HNSCC that were treated with anti-PD-1 ICI therapy in the recurrent or metastatic setting after progression to platinum-based chemotherapy in two independent centers. We analyzed DNA methylation profiles of >850.000 CpG sites in tumor specimens of these patients by Infinium MethylationEPIC microarrays, immune cell density in the tumor microenvironment (CD8, CD3, CD45RO, forkhead box P3 (FOXP3), CD68), PD-1 and programmed cell death ligand 1 (PD-L1) expression by immunohistochemistry, and blood inflammation markers (platelet-to-lymphocyte ratio, leucocyte-to-lymphocyte ratio, monocyte-to-lymphocyte ratio, neutrophil-to-lymphocyte ratio). DNA methylation profiles and immunological markers were bioinformatically and statistically correlated with radiological response to anti-PD-1 ICI.

Results 37 patients with HNSCC (median age of 62 years; range 49–83; 8 (21.6%) women, 29 (78.4%) men) were included (Center 1 N=26, 70.3%; Center 2 N=11, 29.7%). Median number of prior systemic therapies was 1 (range 1–4). Five out of 37 (13.5%) patients achieved an objective response to ICI. Median progression-free survival and median overall survival times were 3.7 months (range 0–22.9) and 9.0 months (range 0–38.8), respectively. Microarray analyses revealed a methylation signature including both hypomethylation and hypermethylation which was predictive for response to ICI and included several genes involved in cancer-related molecular pathways. Over-represented differentially methylated genes between responders and non-responders were associated with 'Axon guidance', 'Hippo signaling', 'Pathways in cancer' and 'MAPK signaling'. A statistically significant correlation of PD-L1 expression and response was present (p=0.0498).

Conclusions Our findings suggest that tumor DNA methylation profiling may be useful to predict response to ICI in patients with HNSCC.

INTRODUCTION

Immune checkpoint inhibitors (ICI) targeting the programmed cell death 1 (PD-1)/programmed cell death ligand 1 (PD-L1) axis have been successfully investigated in recurrent/metastatic (R/M) head and neck squamous cell carcinoma (HNSCC).

The CheckMate 141 and Keynote 040 studies reported superior median overall survival (OS) times of 7.5–8.4 months compared with investigator's choice therapy (5.1 and 6.9 months) in patients with platinum-resistant R/M HNSCC, respectively.[1 2] Based on these findings, nivolumab and pembrolizumab were approved in this setting in most parts of the world. However, only a minority of patients benefit from ICI. The objective response rate (ORR) to single agent ICI (13.3%–14.6%) was low and progression-free survival (PFS) comparable between the treatment arms with and without ICI.[3] While PD-L1 expression has been employed as a potential biomarker for response to ICI in patients with HNSCC, clinical trial data regarding its predictive value are conflicting and discordant. Particularly, the updated long-term analysis of CheckMate

141 showed that PD-L1 negative patients could potentially benefit from ICI as well.[2 4 5] Considering the potential of durable response to ICI, a more precise and personalized biomarker is urgently needed.

Alterations of DNA methylation leading to deregulated transcriptional gene activity are key features of tumorigenesis and affect a variety of signaling pathways.[6–11] Employing methylation profiling could help in reclassification and diagnosis of tumors with a wide spectrum of histologic or molecular subtypes, including brain tumors and sarcomas.[12–16] In addition, certain patterns of DNA methylation may be used as predictive biomarker for therapy response, including immune checkpoint inhibitor therapy as shown in some tumor types.[17–19] To our knowledge, the predictive value of DNA methylation profiles has not been investigated in patients with HNSCC yet.

This study reports DNA methylation profiles of tumors from patients with R/M HNSCC treated with anti-PD-1 ICI in two independent oncology centers. Further, we correlated methylation profiles with tissue-based and blood-based immunological markers as well as therapy response to assess potential new predictive biomarkers for anti-PD-1 ICI therapy in patients with R/M HNSCC.

MATERIAL AND METHODS
Patients' and clinical characteristics
Patients were retrospectively identified from two independent centers (Center 1: Medical University of Vienna, Vienna, Austria; Center 2: Paracelsus Medical University, Salzburg, Austria) according to the following predefined inclusion criteria: age ≥18 years, underlying histologically confirmed HNSCC, application of at least one cycle of an anti-PD-1 ICI antibody (pembrolizumab or nivolumab) for platinum-resistant R/M disease, measurable disease (lesions at least 10×10 mm) on radiological imaging prior to anti-PD-1 ICI antibody therapy start, either at least one radiological restaging under ICI therapy available or occurrence of death before the first radiological restaging could be performed, formalin-fixed paraffin-embedded (FFPE) tumor tissue prior to anti-PD-1 ICI therapy start available. The collected clinical data of patients included baseline patients' characteristics, parameters of systemic inflammation at ICI therapy start (platelet-to-lymphocyte ratio (PLR), leucocyte-to-lymphocyte ratio (LLR), monocyte-to-lymphocyte ratio (MLR), neutrophil-to-lymphocyte ratio (NLR)) as well as survival times were obtained from patient charts. Radiological assessment of response was defined according to theResponse Evaluation Criteria in Solid Tumours for immune-based therapeutics (iRECIST criteria) and performed by independent radiologists from the centers.[20] Objective response was determined by complete response (CR) or partial response (PR) and disease control by CR, PR or stable disease (SD) as best achieved response. Patients who received at least one cycle of anti-PD-1 ICI were evaluable for response assessment. Patients who received one cycle of anti-PD-1 ICI and died before the first restaging during ongoing ICI therapy in case of early progression were determined as non-responders. According to iRECIST criteria, the date of immune unconfirmed progressive disease is regarded as time point of progression if no subsequent restaging followed due to clear clinical progression or death of the patient.[20] Patients were independently treated according to the current good clinical practice guidelines.

Assessment of immune cell subsets and immune-checkpoint expression in the tumor microenvironment by immunohistochemistry
Expression of immune cell subsets (cluster of differentiation 3 (CD3), CD8, CD45RO, FOXP3, CD68) and immune-checkpoint molecules (PD-1, PD-L1) in FFPE tumor tissue samples prior to anti-PD-1 ICI therapy start from either the primary tumor or a metastatic site (excluding lymph node metastases) were assessed by immunohistochemical stainings and semi-automatically analyzed as previously described.[19] Staining antibodies and dilution protocols are shown in online supplemental table 1. Expression of immune cell subsets was described by absolute counts of positively stained cells per square millimeter tumor.

Genome-wide DNA methylation analysis
HNSCC specimens that were sampled before the first application of anti-PD-1 ICI therapy and contained ≥70% of tumor cells as evaluated by local pathologists were selected for the analysis. Genomic DNA was isolated and sodium bisulfite treatment was performed as previously described.[19] High throughput genome-wide DNA methylation analyses were performed with Infinium MethylationEPIC BeadChip microarrays (Illumina, San Diego, California, USA) as previously described.[19] The RnBeads package was used to load raw microarray data (.idat files) into the statistics program R (V.R 4.0.4, R Foundation for Statistical Computing, Vienna, Austria) for initial quality control, pre-processing and differential methylation analysis.[21] Single nucleotide polymorphism (SNP) associated probes, non-specific/cross-hybridizing probes and probes specific for sex chromosomes were excluded from the consecutive analyses. In addition, quality of methylation data were checked using the Greedycut algorithm implemented in RnBeads which iteratively removes all probes and all samples with unreliable measurements ($p > 0.05$) from subsequent analyses.[21] Data normalization was performed using the SWAN algorithm.[22] Differential methylation between groups was calculated by RnBeads as a combined rank score originating from the difference in mean methylation levels of the two groups, the quotient in mean methylation and a two-sided Welch t-test assessing whether the methylation values in the two groups originate from distinct distributions. The top 1000 differentially methylated CpG sites were selected for further evaluation. Analyses of gene ontology (GO) and KEGG pathway enrichment were conducted with the

WebGestalt tool.[23] Heatmaps were generated using the ClustVis tool.[24]

Assessment of copy number variations

Copy number variations (CNVs) were evaluated from the .idat files retrieved from the Infinium MethylationEPIC BeadChip microarrays using the R package conumee implemented at https://www.molecularneuropathology. org/mnp, as previously described.[19]

Statistics

The PFS and OS from anti-PD-1 ICI therapy start were determined from first application until progression of disease or death. Patients that did not progress nor die by the time of data cut-off were censored at their last follow-up visit. The Mann-Whitney U test and the Kruskal-Wallis test were used to test for differences between groups. Statistical significance was indicated by a two-tailed p value≤0.05. Multiple testing was corrected using the Bonferroni method. Statistical analyses were performed with Statistical Package for the Social Sciences (SPSS) V.23.0 software (SPSS, Chicago, Illinois, USA) and standard R functions (V.R 4.0.4, R Foundation for Statistical Computing, Vienna, Austria).

RESULTS

Characteristics of patients

Thirty-seven patients (8 women, 21.6%; 29 men, 78.4%) with a median age of 62 (range 49–83) years were included in the analysis. Patients had received a median number of 1 (range 1–4) prior systemic therapies. Thirty-four out of 37 (91.9%) patients received a platinum-based chemotherapy prior to ICI while 3/37 (8.1%) patients were not eligible for a platinum-based therapy due to a low performance status or comorbidities. Twenty-four out of 37 (64.9%) patients received cetuximab, 9/37 (24.3%) patients received a taxane and 17/37 (45.9%) of patients received 5-FU before ICI therapy start. All responders (5/5 patients) had received a platinum-based therapy prior to ICI start, two responders had received cetuximab, one responder had received 5-FU and none of the responders had received taxanes prior to ICI start. There was no significant difference in the number of prior received systemic therapies between responders and non-responders (p>0.05). Twenty-nine patients (78.4%) received the anti-PD-1 ICI antibody nivolumab and eight patients (21.6%) received pembrolizumab. The median number of anti-PD-1 ICI cycles received was seven (range 1–45) while responders received a median number of 21 cycles and non-responders a median number of 6 cycles of ICI therapy. The higher overall number of cycles applied in responders is expected, as the ICI inhibitor therapy is regularly terminated at the time of tumor progression. The methylation signature is analyzed from tumor tissues obtained before start of ICI therapy. One of 37 (2.7%) patients of the cohort achieved a CR and 4/37 (10.8%) patients achieved a PR under anti-PD-1 therapy, which

results in an ORR of 13.5%. Five of 37 (13.5%) patients achieved a SD as best response, which results in a clinical benefit rate of 27.0% (figure 1A and B). The median PFS and OS from anti-PD-1 ICI therapy start were 3.7 (0–22.9) months and 9.0 (0–38.8) months, respectively (figure 1D and E). online supplemental figure 1 and online supplemental table 2) show detailed information on the number of received ICI, time point of restagings and best achieved responses per patient. Median PFS from ICI therapy start was significantly longer in responders versus non-responders (10.2 months vs 3.3 months, p=0.042, log-rank test) while OS from ICI therapy start was numerically longer in responders versus non-responders (22.8 months vs 7.2 months, p>0.05, long-rank test; figure 1F and G). The median duration of follow-up from the start of treatment for all patients was 8.1 months, while responders showed a median duration of follow-up of 22.6 months and non-responders showed a median duration of follow-up of 6.8 months. Clinical patients' characteristics are listed in table 1.

Correlation of immune cell subsets in the tumor microenvironment as well as blood-based parameters of systemic inflammation with anti-PD-1 therapy response

Twenty of 37 (54.1%) patients showed PD-L1 expression on tumor cells (PD-L1 ≥1). All responders (5/5, 100%) showed PD-L1 expression with a range of 1–100 intensity of PD-L1 expression while 15/32 (46.9%) of non-responders showed PD-L1 expression (0–100 intensity of PD-L1 expression). Expression of PD-L1 significantly correlated with therapy response (Fisher's exact test, p=0.0498, figure 1C). Densities of investigated immune cells (CD8 +tumor-infiltrating lymphocytes (TILs), CD3 +TILs, CD45RO+TILs, FOXP3 +TILs, PD-1 +TILs, CD68 +TILs) and markers of systemic inflammation (NLR, LLR, PLR, MLR) are shown in table 2. No association of density of other investigated immune cells or systemic inflammation markers with response to anti-PD-1 ICI treatment was seen (Mann-Whitney U test, p>0.05; online supplemental figure 2).

Profiling of tumor DNA methylation patterns and correlation with response to anti-PD-1 ICI therapy

To investigate if the methylation profiles of patients with HNSCC differ between patients who achieved an objective response to anti-PD-1 ICI therapy (N=5) and patients who did not achieve an objective response to anti-PD-1 ICI therapy (N=32), we conducted Illumina MethylationEPIC microarray analyses including 866895 probes. Initial quality control of microarray data resulted in exclusion of 139,721 probes overlapping with SNPs, 34,264 cross-reactive probes and 5406 probes with unreliable measurements, 1128 non-CpG probes and 16,243 sex chromosome specific probes. Overall, data from 670,133 probes were normalized and used for further statistical evaluation (figure 2A). Principal component analysis based on these data revealed variability within the patients with HNSCC who did not respond to ICI while patients with HNSCC
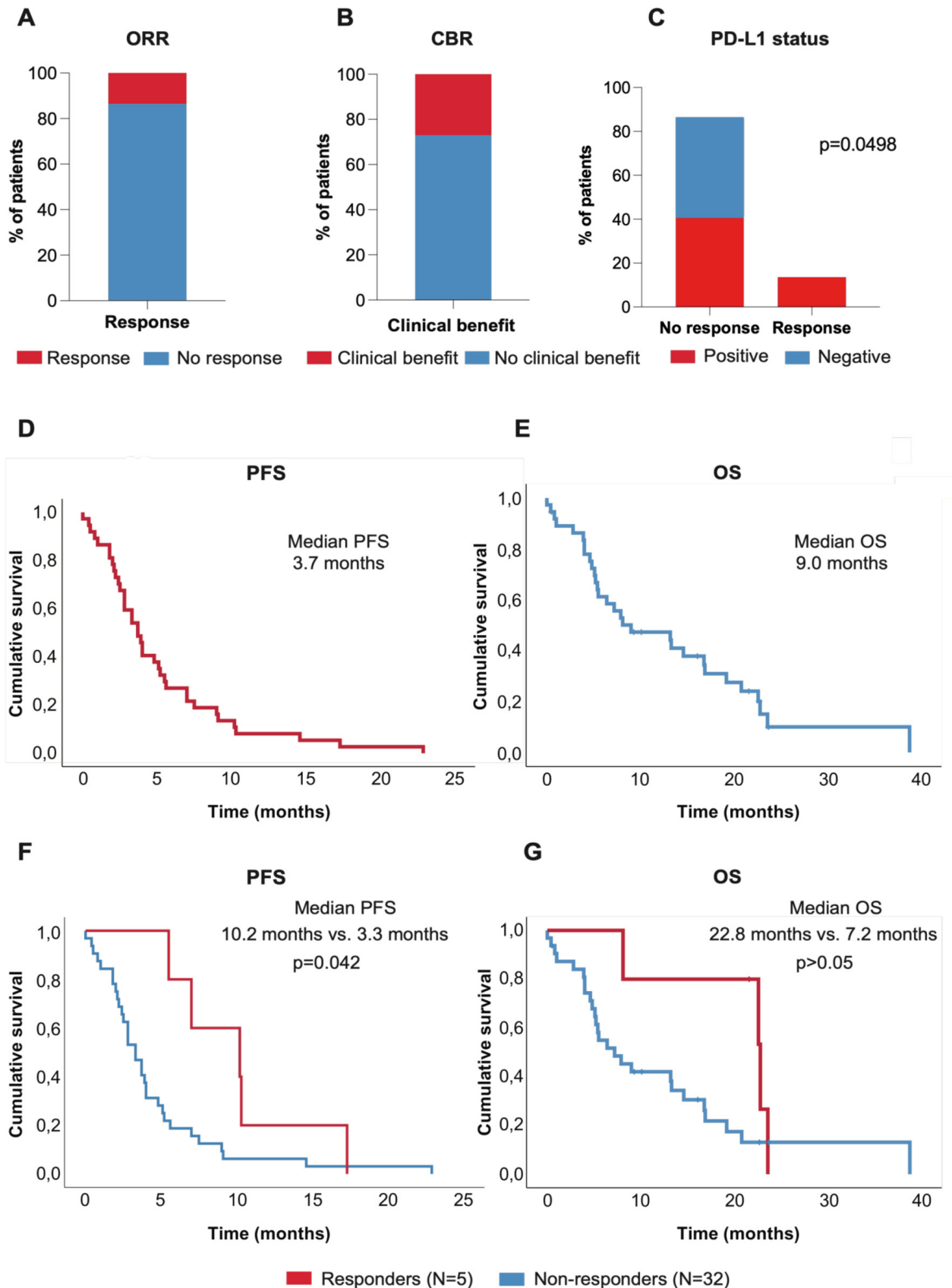
Figure 1 (A) Objective response rate (ORR) and (B) clinical benefit rate (CBR) in the study cohort. (C) Bar graph depicting the fraction of PD-L1 positive and negative patients in responders and non-responders to ICI. Figures (D) and (E) show progression-free survival (PFS) as well as overall survival (OS) in months from start of anti-PD-1 ICI therapy in the total study cohort. Figures (F) and (G) show PFS and OS from anti-PD-1 ICI therapy start in responders vs non-responders to ICI. ICI, immune checkpoint inhibitors; PD-1, programmed cell death 1; PD-L1, programmed cell death ligand 1.

Table 1 Patients' characteristics

Patients' characteristics	N=37	%
Center 1	26	70.3
Center 2	11	29.7
Gender		
Female	8	21.6
Male	29	78.4
Age at anti-PD-1 ICI therapy start, in years		
Median (range)	62 (49–83)	
Location of primary tumor		
Oropharynx	14	37.8
Hypopharynx	5	13.5
Larynx	4	10.8
Oral cavity	9	24.3
Others	5	13.5
HPV status in oropharyngeal carcinomas (=14)		
Positive	5	35.7
Negative	4	28.6
Missing	5	35.7
p16 status in oropharyngeal carcinomas (=14)		
Positive	6	42.9
Negative	4	28.6
Missing	4	28.6
Smoking status		
Active/former smoker	32	86.5
Never smoker	5	13.5
Primary therapy		
Surgery±adjuvant (chemo) radiation	18	48.6
(Chemo)radiation only	17	45.9
Systemic therapy only	2	5.4
Therapy lines prior to anti-PD-1 therapy		
Median (range)	1 (1–4)	
ECOG at anti-PD-1 ICI therapy start		
0	12	32.4
1	18	48.6
2	7	18.9
Anti-PD-1 ICI agent		
Pembrolizumab	8	21.6
Nivolumab	29	78.4
Number of anti-PD-1 ICI therapy applications		
Median (range)	7 (1–45)	

Continued

Table 1 Continued

Patients' characteristics	N=37	%
PFS (from anti-PD-1 ICI therapy start), in months		
Median (range)	3.7 (0–22.9)	
OS (from anti-PD-1 ICI therapy start), in months		
Median (range)	9 (0–38.8)	
OS (from primary tumor diagnosis), in months		
Median (range)	36.6 (7.6–193.4)	
Deceased		
Yes	30	81.1
No	7	18.9

ECOG, Eastern Cooperative Oncology Group; ICI, immune checkpoint inhibitors ; OS, overall survival; PD-1, programmed cell death 1 ; PFS, progression-free survival.

who responded to this type of treatment cluster in closer proximity (figure 2B).

In a next step, we tested for methylation differences between responding and non-responding patients to ICI using RnBeads. This analysis resulted in the identification of 63,294 differentially methylated CpG sites. To focus on the strongest methylation differences, we selected the top 1000 differentially methylated CpG sites (DMP) for further evaluation. These DMPs can be divided into 688 hypomethylated DMPs and 312 hypermethylated DMPs

Table 2 Inflammation characteristics

Inflammation characteristics	N=37	%
Tumor PD-L1 expression		
Positive	20	54.1
Negative	17	45.9
	Median	**Range**
CD3 +TILs/mm^2 tumor	827.25	1.68–8811.74
CD8 +TILs/mm^2 tumor	533.77	5.34–11 528.43
CD45RO+TILs/mm^2 tumor	485.63	45.65–3696.09
FOXP3 +TILs/mm^2 tumor	258.67	7.68–1894.57
PD-1+TILs/mm^2 tumor	107.35	0–1220.61
CD68 +TILs/mm^2 tumor	528.62	100.17–1803.55
NLR (missing n=1)	7.26	2.26–91.83
LLR (missing n=1)	9.58	3.98–101.0
PLR (missing n=1)	390.88	96.43–3116.67
MLR (missing n=1)	0.75	0.28–6.0

FOXP3, forkhead box P3 ; LLR, leucocyte-to-lymphocyte ratio ; MLR, monocyte-to-lymphocyte ratio ; mm^2, millimeter; NLR, neutrophil-to-lymphocyte ratio ; PD-1, programmed cell death 1 ; PD-L1, programmed cell death ligand 1 ; PLR, platelet-to-lymphocyte ratio ; TIL, tumor-infiltrating lymphocyte .
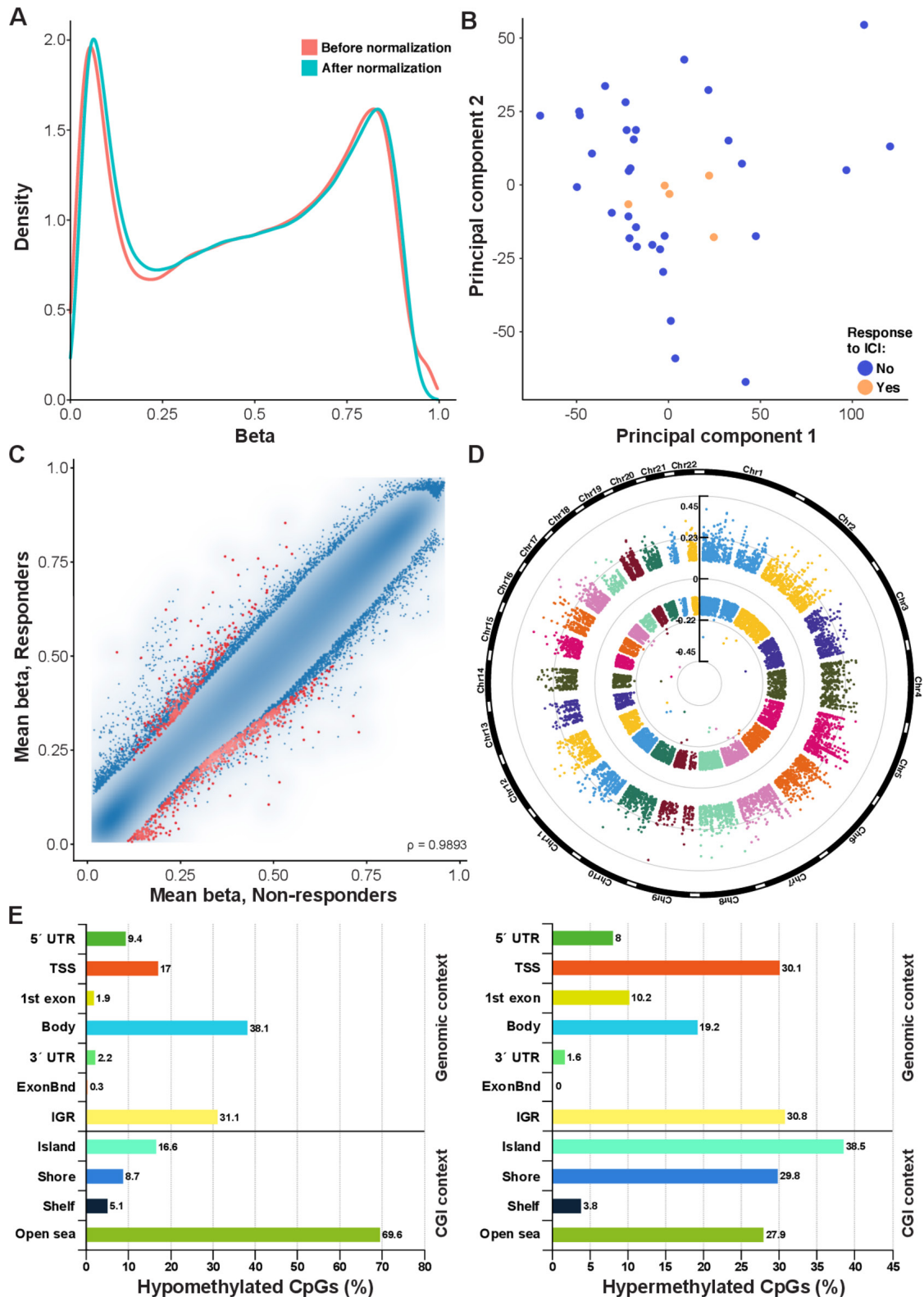
Figure 2 DNA methylation profiling of patients with HNSCC treated with ICI. (A) Comparison of β values before and after normalization. Both distributions are estimated by randomly sampling 1,000,000 values in each group. (B) Principal component analysis of HNSCC samples based on β values of 670,133 probes. Blue and orange colored dots represent non-responders (N) and responders (R) to ICI, respectively. (C) Scatter plot summarizing differences of methylation between responding and non-responding patients to anti-PD-1 ICI. Red dots indicate the top 1000 differentially methylated CpG sites. (D) Chromosomal distribution of differentially methylated CpG sites. β values differences between responders and non-responders to ICI are shown. (E) Percentage of differentially methylated CpG sites located in certain genomic and CpG island associated regions. cGI, CpG island; ExonBnd, exon boundary; HNSCC, head and neck squamous cell carcinoma; ICI, immune checkpoint inhibitors; IGR, intergenomic region; PD-1, programmed cell death 1; UTR, untranslated region; TSS, transcription start site.

in responders compared with non-responders (figure 2C, (online supplemental table 3). DMPs that were hypomethylated and hypermethylated were evenly distributed among all chromosomes as shown in figure 2D. Mapping of these DMPs to their genomic position in the context of gene-associated regions, 38.1% of hypomethylated DMPs were found in gene bodies, 31.1% in intergenic regions, 17% in transcriptional start sites, 9.4% in 5' untranslated regions (UTRs), 2.2% in 3' UTRs, 0.3% in exon boundaries and 1.9% in first exons. These frequencies were similar for hypermethylated DMPs, except of higher transcription start site/first exon frequencies and a lower gene body frequency (figure 2E). The association of hypomethylated DMPs with CpG islands (CGI), shore (2 kb regions flanking CGIs), shelf (2 kb regions of flanking shore regions) and open sea regions revealed a non-CGI DMP over-representation (69.6%). There was a lower frequency of hypermethylated non-CpG island DMPs (27.9%, figure 2E). Additionally, the distributions of hypomethylated and hypermethylated CpG island associated DMPs were 16.6% and 38.5% for CGIs, 8.7% and 29.8% for shore regions, and 5.1% and 3.8% for shelf regions, respectively.

Cluster analysis of HNSCC samples using the top 1000 DMPs yielded four main clusters of which one included all of the responders to anti-PD-1 ICI therapy and the other ones contained only the non-responders (figure 3A). Clustering of the samples was associated only with response to anti-PD-1 ICI therapy and no other association with center, gender, type of therapy, tumor location, smoking status, HPV status, p16 protein expression and immune cell infiltration was seen. Of note, methylation of the vast majority of the 1000 DMPs was relatively homogeneous (mean variance: 0.004) within the responder cluster. By contrast, mean variances of methylation values within the other three clusters were 4.3–7.1 times higher compared with cluster one. After testing if these clusters may be prognostically dissent we did not see a PFS/OS difference between the three non-responder clusters (C2, C3 and C4) but only a trend towards better PFS/OS of the responder cluster (C1; online supplemental figure 3).

Functional characterization of differentially methylated genes

To determine the biological meaning of our predictive methylation signature the 1000 DMPs described above were mapped to 724 genes. These genes were used for subsequent pathway enrichment analyses. Regarding KEGG pathways, differentially methylated genes between responders and non-responders were associated with 'Axon guidance' (hsa04360, false discovery rate (FDR)=0.027; e.g. *BMPR1B*, *CAMK2D*, *EPHNA6*, *NTNG1*), 'Hippo signaling' (hsa04390, FDR=0.027; for example, *AFP*, *BMP7*, *GLI1*), 'Pathways in cancer' (hsa05200, FDR=0.027; for example, *MAPK10*, *IL2RA*, *IGF1R*, *AKT3*, *MLH1*, *COL4A1*) and 'MAPK signaling' (hsa04010, FDR=0.028; for example, *TAOK3*, *STK3*, *IL1RAP*, *MAP3K1*) were over-represented (figure 3B, (online supplemental table 4 and 5). The difference in methylation pattern of

'Pathways in cancer' members in responders and non-responders to ICI of our patient with HNSCC cohort is shown in figure 3B. By GO enrichment analysis, we found a statistically significant over-representation of factors involved in many developmental processes, for example, cell growth, fibroblast proliferation, vascular endothelial growth factor receptor signaling pathway and many more (online supplemental table 6).

CNV in HNSCCs

Because CNVs are frequently found in HNSCCs we investigated the difference of CNVs in responders and non-responders to ICI.[25] A various extent of CNVs was detected in the tumor samples which is illustrated in online supplemental figures 4 and 5. Some of the HNSCC specimens contained no or only a low amount of CNVs, while others showed many CNVs. By comparing CNV patterns between responders and non-responders to ICI we did not see distinct differences indicating that CNVs are not suited to differentiate between responders and non-responders to anti-PD-1 ICI therapy in patients with HNSCC.

DISCUSSION

ICI have high therapeutic potential, as in contrast to most chemotherapy and targeted therapies durable responses in patients with various solid tumor types including HNSCC have been occasionally observed.[26–28] Unfortunately, the ORR to ICI treatment is low in patients with R/M HNSCC. In the present cohort the ORR was only 13.5%, similar to the ones reported in recent phase III trials.[1] [2] Although ICI therapy bears the potential of durable responses, immune-related side effects of the treatment have to be considered. Thus, an accurate biomarker to select patients is urgently needed. In the present study we analyzed more than 850 thousand CpG sites in patients with R/M HNSCC treated with anti-PD-1 therapy after platinum-failure in order to investigate the predictive potential of DNA methylation profile as a novel biomarker for ICI treatment.

The methylation profile of responding and non-responding HNSCC tumors in the present cohort showed both hypomethylation and hypermethylation and correlated with ICI response. Other tissue-based parameters such as TIL density did not correlate with ICI response in our cohort. In contrast, previous studies have shown a positive correlation of TIL density and ICI therapy response in some tumor types.[29–32] However, different cancers may differently respond to ICI although showing similar TIL compositions, indicating a complex interplay of cancer and immune cells.[33] A possible explanation for not seeing a correlation in our cohort could be due to different prior therapy modalities including radiotherapy and systemic therapies, which were shown to influence the inflammatory microenvironment composition.[34] TIL density alone has not shown consistent predictive potential so far and is therefore not used routinely as a biomarker in the clinical practice. However, a strong
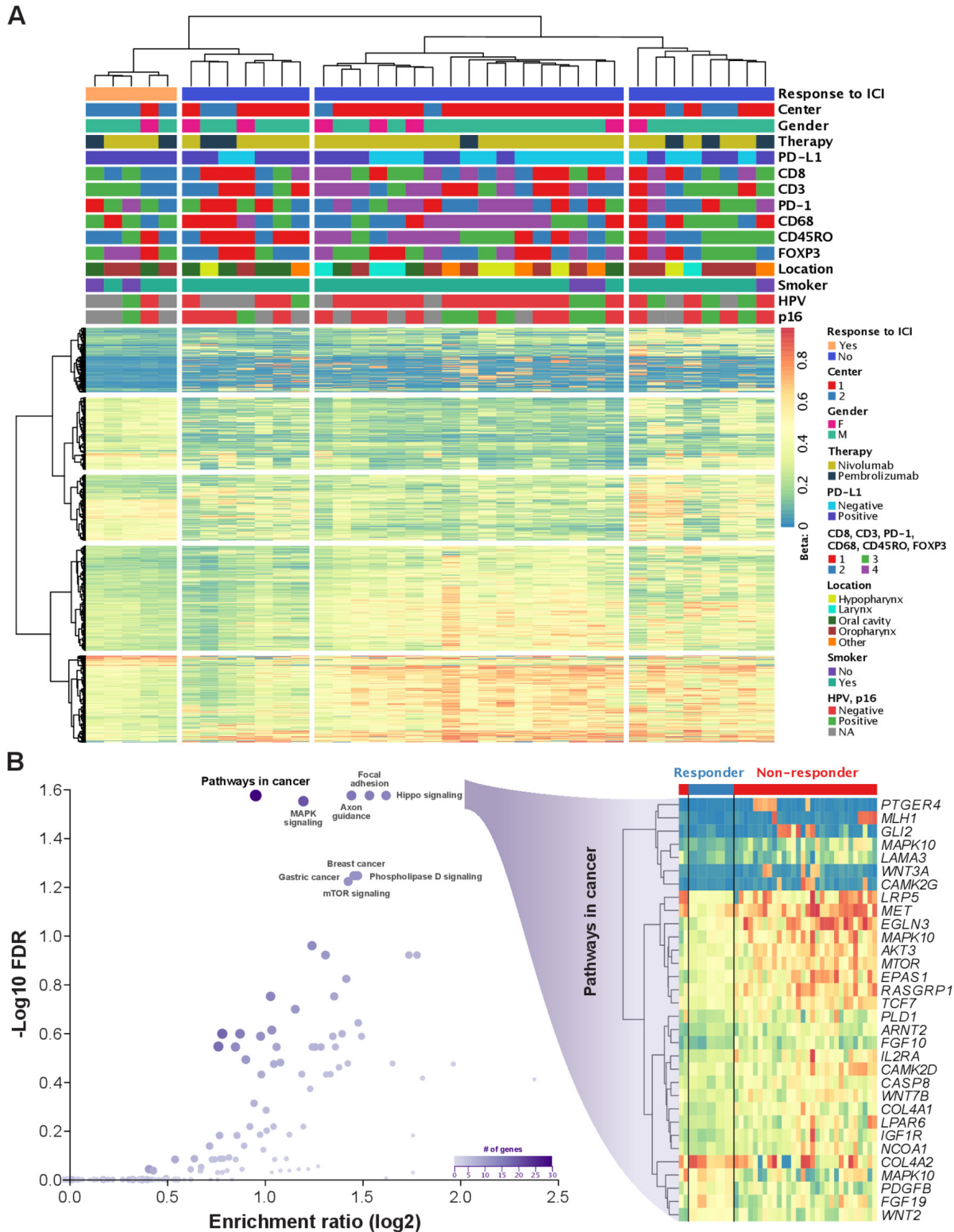
Figure 3 Comparison of methylation differences with clinical variables and pathway enrichment analyses. (A) Heatmap illustrating methylation values of 1000 CpG sites in 37 head and neck squamous cell carcinoma specimens. Patients' characteristics including response to anti-PD-1 ICI, center, gender, type of therapy, tumor location, smoking status, HPV status, p16 protein expression and expression of various immune parameters are shown according to the legend next to the heatmap. Rows represent unique CpG sites and columns represent unique patient samples. Colors shown in the heatmap reflect β values without centering/scaling. (B) Results from KEGG pathway enrichment analysis are shown in the left panel. Each dot indicates a unique KEGG pathway. Methylation values of genes involved in the KEGG category 'pathways in cancer' are summarized in the heatmap (right). The responder (blue) columns were stretched for better visibility. Heatmap colors reflect β values without centering/scaling. FOXP3, forkhead box P3; ICI, immune checkpoint inhibitors; PD-1, programmed cell death 1; PD-L1, programmed cell death ligand 1; FDR false discovery rate.

prognostic role of TIL densities has been described in different cancers including HNSCC, thus underlining the importance of the inflammatory tumor microenvironment composition for immune responses.[35]

Although, PD-L1 positivity correlated with therapy response in the present cohort, a large fraction of non-responding patients was also PD-L1 positive, limiting the predictive accuracy of PD-L1 expression. Furthermore, previous studies reported responses to PD-1/PD-L1 targeting therapies also in patients with PD-L1-negative HNSCC, thus underlining the suboptimal predictive value of this biomarker.[36] The investigation of DNA methylation profiles, however, allowed a distinction between responders and non-responders to anti-PD-1 ICI therapy in the present study. Studies of our own group, as well as from others, previously postulated an association of the DNA methylation profile with response to ICI for patients with sarcoma and patients with non-small cell lung cancer treated with ICI.[19 37] To the best of our knowledge, we show here for the first time a potential value of DNA methylation signatures as a predictive biomarker in HNSCC tumors, which should be confirmed in further studies.

Pathway enrichment analyses based on genes included in our differential DNA methylation signature between responding and non-responding tumors identified several affected molecular pathways. Here, genes associated with 'Axon guidance', 'Hippo signaling', 'Pathways in cancer' and 'MAPK signaling' were differentially methylated between responding and non-responding tumors. Although no exceptional inflammation pathway showed differential methylation, inflammation associated genes are included in the identified pathways. Interleukin 2 (IL-2) receptor alpha is included in the 'Pathways in cancer' (figure 3B) and was previously postulated to impact the tumor specific immune response. Preclinical data suggest that IL-2 treatment enhances cytotoxic T lymphocytes and improves the intratumoral T cell composition of effector and regulatory T cells.[38 39] On the other side, IL-2 receptor alpha overexpression in tumor cells was associated with tumor progression and poor outcome in a head and neck cancer cell line.[40] Another example of a differentially methylated gene associated with 'Pathways in cancer' is prostaglandin E receptor 4 (PTGER4) (figure 3B), which is associated with immune suppression in the tumor microenvironment.[41] In preclinical studies the inhibition of PTGER4 has been shown to decline tumor growth, inhibit the immune-suppressive function of prostaglandin E2 and was proposed for combinational immunotherapy with PD-1-axis-targeting agents.[41 42] Interestingly, methylated PTGER4 of blood samples has been shown to be a useful marker for monitoring therapy response in patient with stage IV lung cancer receiving chemotherapy, radiotherapy and chemotherapy or tyrosine kinase inhibitors since the levels of methylated PTGER4 significantly decreased in patients who achieved a PR.[43] Our data, therefore, imply that several genes involved in immune responses against cancer are affected by differential methylation between responders and non-responders and emphasize further research on these differentially methylated pathways and their potential role as future therapy targets.

Importantly, limitations of this study need to be recognized to correctly interpret our data. We could show the potential of methylation patterns as biomarker for ICI therapy response. However, this observation by now was only investigated in some cancer types, for example, in this cohort in patients with HNSCC and previously in patients with sarcoma and patients with lung cancer.[19 37 44 45] Therefore, the methylome of other tumor entities being treated with ICI needs to be investigated as well. Furthermore, the sample size in this study is limited, however, we included patients from two independent oncology centers forming a multi-institutional well-defined patient cohort. The observed response rate in the cohort of 13.5% reflects the response rate in prospective trials of ICI treatment in HNSCC, underscoring that our cohort is representative.[1 2] Indeed, responders to ICI achieved a significantly better PFS compared with non-responders, however, due to the limited sample size we only observed a numerically better OS in responders in our patient cohort of patients with R/M HNSCC. Another limitation of our study is the retrospective study design, although clear inclusion and exclusion criteria as well as a precise documentation of patient histories were obliged for this analysis. Due to clinical indications in our patients the first radiological response assessments were performed after one to seven treatment cycles which generates a variability of treatment duration in our patient cohort. Radiological response assessment was performed early if clinically indicated due to a strong clinical suspicion of disease progression, that is, due to the development of new symptoms, which is a common approach in the real-world therapy setting. However, given the current lack of reliable predictive biomarker in HNSCC for ICI treatment our data should be validated in future and larger investigations. Ideally this validation could be performed retrospectively with patient samples from large phase 3 clinical trials of ICI in HNSCC. This set up would allow to validate the predictive potential of the observed methylation signature in a well-defined patient cohort. Further, prospective validation within an upcoming trial, for example, as inclusion or stratification factor would further direct the development of methylation signatures as a biomarker for ICI response.

In conclusion, this data indicates that DNA methylation profiles may be usable as a biomarker for response to anti-PD-1 ICI therapy in HNSCC. Further studies are needed to validate our findings in order to establish a robust methylation IO classifier as biomarker for ICI therapy response.

Author affiliations
[1]Department of Medicine I, Division of Oncology, Medical University of Vienna, Vienna, Austria
[2]Department of Medicine I, Christian Doppler Laboratory for Personalized Immunotherapy, Medical University of Vienna, Vienna, Austria

3Laboratory for Immunological and Molecular Cancer Research, Department of Internal Medicine III with Hematology, Medical Oncology, Hemostaseology, Infectious Diseases, Rheumatology, Oncologic Center, Paracelsus Medical University Salzburg, Salzburg, Austria
4Department of Biomedical Imaging and Image-guided Therapy, Medical University of Vienna, Vienna, Austria
5Department of Pathology, Medical University of Vienna, Vienna, Austria

Patient consent for publication Not applicable.

Ethics approval This study involves human participants and was approved by ethics committee of the Medical University of Vienna, ID 1381/2019 and ethics committee of Salzburg, ID 1190/2020. Not applicable due to the retrospective study design.

Provenance and peer review Not commissioned; externally peer reviewed.

Data availability statement Data are available upon reasonable request. All data relevant to the study are included in the article or uploaded as supplementary information. Relevant additional data can be shared on request to the authors. Data are available upon reasonable request.

ORCID iDs
Angelika Martina Starzer http://orcid.org/0000-0001-5867-8461
Gerwin Heller http://orcid.org/0000-0001-8742-5631
Anna Sophie Berghoff http://orcid.org/0000-0001-9379-6797

REFERENCES

1 Ferris RL, Blumenschein G, Fayette J, *et al*. Nivolumab for recurrent squamous-cell carcinoma of the head and neck. *N Engl J Med Overseas Ed* 2016;375:1856–67
2 Cohen EEW, Soulières D, Le Tourneau C, *et al*. Pembrolizumab versus methotrexate, docetaxel, or cetuximab for recurrent or metastatic head-and-neck squamous cell carcinoma (KEYNOTE-040): a randomised, open-label, phase 3 study. *Lancet* 2019;393:156–67.
3 Burtness B, Harrington KJ, Greil R, *et al*. Pembrolizumab alone or with chemotherapy versus cetuximab with chemotherapy for recurrent or metastatic squamous cell carcinoma of the head and neck (KEYNOTE-048): a randomised, open-label, phase 3 study. *Lancet* 2019;394:1915–28.
4 Bauml J, Seiwert TY, Pfister DG, *et al*. Pembrolizumab for platinum- and cetuximab-refractory head and neck cancer: results from a single-arm, phase II study. *J Clin Oncol* 2017;35:1542–9.
5 Ferris RL, Blumenschein G, Fayette J, *et al*. Nivolumab vs investigator's choice in recurrent or metastatic squamous cell carcinoma of the head and neck: 2-year long-term survival update of CheckMate 141 with analyses by tumor PD-L1 expression. *Oral Oncol* 2018;81:45–51.
6 Abeshouse A, Adebamowo C, Adebamowo SN. Comprehensive and integrated genomic characterization of adult soft tissue sarcomas. *Cell* 2017;171:950–65.
7 Chiba T, Yokosuka O, Arai M, *et al*. Identification of genes up-regulated by histone deacetylase inhibition with cDNA microarray and exploration of epigenetic alterations on hepatoma cells. *J Hepatol* 2004;41:436–45.
8 Tian W, Li Y, Zhang J, *et al*. Combined analysis of DNA methylation and gene expression profiles of osteosarcoma identified several prognosis signatures. *Gene* 2018;650:7–14.
9 Irizarry RA, Ladd-Acosta C, Wen B, *et al*. The human colon cancer methylome shows similar hypo- and hypermethylation at conserved tissue-specific CpG island shores. *Nat Genet* 2009;41:178–86.
10 Li C, Xiong W, Liu X, *et al*. Hypomethylation at non-CpG/CpG sites in the promoter of HIF-1α gene combined with enhanced H3K9Ac modification contribute to maintain higher HIF-1α expression in breast cancer. *Oncogenesis* 2019;8:26.
11 Truong M, Yang B, Wagner J, *et al*. Analysis of promoter non-CG methylation in prostate cancer. *Epigenomics* 2013;5:65–71.
12 Sahm F, Schrimpf D, Stichel D, *et al*. Dna methylation-based classification and grading system for meningioma: a multicentre, retrospective analysis. *Lancet Oncol* 2017;18:682–94.
13 Capper D, Jones DTW, Sill M, *et al*. Dna methylation-based classification of central nervous system tumours. *Nature* 2018;555:469–74.
14 Kommoss FKF, Stichel D, Schrimpf D, *et al*. Dna methylation-based profiling of uterine neoplasms: a novel tool to improve gynecologic cancer diagnostics. *J Cancer Res Clin Oncol* 2020;146:97–104.
15 Weidema ME, van de Geer E, Koelsche C, *et al*. Dna methylation profiling identifies distinct clusters in angiosarcomas. *Clin Cancer Res* 2020;26:93–100.
16 Koelsche C, Schrimpf D, Stichel D, *et al*. Sarcoma classification by DNA methylation profiling. *Nat Commun* 2021;12:498.
17 Lauss M, Ringnér M, Karlsson A, *et al*. DNA methylation subgroups in melanoma are associated with proliferative and immunological processes. *BMC Med Genomics* 2015;8:73.
18 Sigin VO, Kalinkin AI, Kuznetsova EB, *et al*. DNA methylation markers panel can improve prediction of response to neoadjuvant chemotherapy in luminal B breast cancer. *Sci Rep* 2020;10:9239.
19 Starzer AM, Berghoff AS, Hamacher R, *et al*. Tumor DNA methylation profiles correlate with response to anti-PD-1 immune checkpoint inhibitor monotherapy in sarcoma patients. *J Immunother Cancer* 2021;9:e001458.
20 Seymour L, Bogaerts J, Perrone A, *et al*. iRECIST: guidelines for response criteria for use in trials testing immunotherapeutics. *Lancet Oncol* 2017;18:e143–52.
21 Müller F, Scherer M, Assenov Y, *et al*. RnBeads 2.0: comprehensive analysis of DNA methylation data. *Genome Biol* 2019;20:55.
22 Maksimovic J, Gordon L, Oshlack A. Swan: Subset-quantile within array normalization for illumina infinium HumanMethylation450 BeadChips. *Genome Biol* 2012;13:R44.
23 Tsujimura T, Takase O, Yoshikawa M, *et al*. Controlling gene activation by enhancers through a drug-inducible topological insulator. *Elife* 2020;9:1–37.
24 Metsalu T, Vilo J. ClustVis: a web tool for visualizing clustering of multivariate data using principal component analysis and heatmap. *Nucleic Acids Res* 2015;43:W566–70.

25 Yang J, Chen Y, Luo H, *et al*. The landscape of somatic copy number alterations in head and neck squamous cell carcinoma. *Front Oncol* 2020;10:321.

26 de Marinis F, Ciardiello F, Baas P, *et al*. 30 Immunotherapy in advanced NSCLC-from the 'tsunami' of therapeutic knowledge to a clinical practice algorithm: results from an international expert panel meeting of the Italian Association of Thoracic Oncology (AIOT). *ESMO Open* 2018;3:e000298.

27 Motzer RJ, Escudier B, McDermott DF, *et al*. Nivolumab versus everolimus in advanced renal-cell carcinoma. *N Engl J Med* 2015;373:1803–13.

28 Schmid P, Adams S, Rugo HS, *et al*. Atezolizumab and nab-paclitaxel in advanced triple-negative breast cancer. *N Engl J Med* 2018;379:2108–21.

29 Paijens ST, Vledder A, de Bruyn M, *et al*. Tumor-Infiltrating lymphocytes in the immunotherapy era. *Cell Mol Immunol* 2021;18:842–59.

30 Taube JM, Klein A, Brahmer JR, *et al*. Association of PD-1, PD-1 ligands, and other features of the tumor immune microenvironment with response to anti-PD-1 therapy. *Clin Cancer Res* 2014;20:5064–74.

31 Outh-Gauer S, Alt M, Le Tourneau C, *et al*. Immunotherapy in head and neck cancers: a new challenge for immunologists, pathologists and clinicians. *Cancer Treat Rev* 2018;65:54–64.

32 Thommen DS, Koelzer VH, Herzig P, *et al*. A transcriptionally and functionally distinct PD-1$^+$ CD8$^+$ T cell pool with predictive potential in non-small-cell lung cancer treated with PD-1 blockade. *Nat Med* 2018;24:994–1004.

33 Teng MWL, Ngiow SF, Ribas A, *et al*. Classifying cancers based on T-cell infiltration and PD-L1. *Cancer Res* 2015;75:2139–45.

34 Tabachnyk M, Distel LVR, Büttner M, *et al*. Radiochemotherapy induces a favourable tumour infiltrating inflammatory cell profile in head and neck cancer. *Oral Oncol* 2012;48:594–601.

35 Solomon B, Young RJ, Bressel M. Prognostic Significance of PD-L1(+) and CD8(+) Immune Cells in HPV(+) Oropharyngeal Squamous Cell Carcinoma. *Cancer Immunol Res* 2018;6:295–304.

36 Davis AA, Patel VG. The role of PD-L1 expression as a predictive biomarker: an analysis of all US food and drug administration (FDA) approvals of immune checkpoint inhibitors. *J Immunother Cancer* 2019;7:278.

37 Duruisseaux M, Martínez-Cardús A, Calleja-Cervantes ME, *et al*. Epigenetic prediction of response to anti-PD-1 treatment in non-small-cell lung cancer: a multicentre, retrospective analysis. *Lancet Respir Med* 2018;6:771–81.

38 Sun Z, Ren Z, Yang K, *et al*. A next-generation tumor-targeting IL-2 preferentially promotes tumor-infiltrating CD8$^+$ T-cell response and effective tumor control. *Nat Commun* 2019;10:3874.

39 Hannani D, Vétizou M, Enot D, *et al*. Anticancer immunotherapy by CTLA-4 blockade: obligatory contribution of IL-2 receptors and negative prognostic impact of soluble CD25. *Cell Res* 2015;25:208–24.

40 Kuhn DJ, Smith DM, Pross S, *et al*. Overexpression of interleukin-2 receptor alpha in a human squamous cell carcinoma of the head and neck cell line is associated with increased proliferation, drug resistance, and transforming ability. *J Cell Biochem* 2003;89:824–36.

41 Peng S, Hu P, Xiao Y-T. Single-Cell analysis reveals EP4 as a target for restoring T-cell infiltration and sensitizing prostate cancer to immunotherapy. clin cancer Res an off J am Assoc cancer Res. *United States* 2022;28:552–67.

42 Take Y, Koizumi S, Nagahisa A. Prostaglandin E receptor 4 antagonist in cancer immunotherapy: mechanisms of action. *Front Immunol* 2020;11:324.

43 Zhang Y, Huang J, Zou Q, *et al*. Methylated PTGER4 is better than CA125, CEA, Cyfra211 and NSE as a therapeutic response assessment marker in stage IV lung cancer. *Oncol Lett* 2020;19:3229–38.

44 Kim JY, Choi JK, Jung H. Genome-Wide methylation patterns predict clinical benefit of immunotherapy in lung cancer. *Clin Epigenetics* 2020;12:119.

45 Seremet T, Koch A, Jansen Y, *et al*. Molecular and epigenetic features of melanomas and tumor immune microenvironment linked to durable remission to ipilimumab-based immunotherapy in metastatic patients. *J Transl Med* 2016;14:232.